Negative Ion Beam production and Transport via the LEBT of the HV injector prototype

O. Sotnikov, Yu. Belchenko, P. Deichuli, A.A. Ivanov, A. Sanin,

Budker Institute of Nuclear Physics, Novosibirsk, Russia

- **BINP Negative-ion based Neutral Beam Injector**
- **Source and beam transport line**
- **Beam transport through LEBT**
- **NI beam separation from accompanying groups of fast atoms**

NIBS 2018, September 6, Novosibirsk

Negative-ion based Neutral Beam Injector

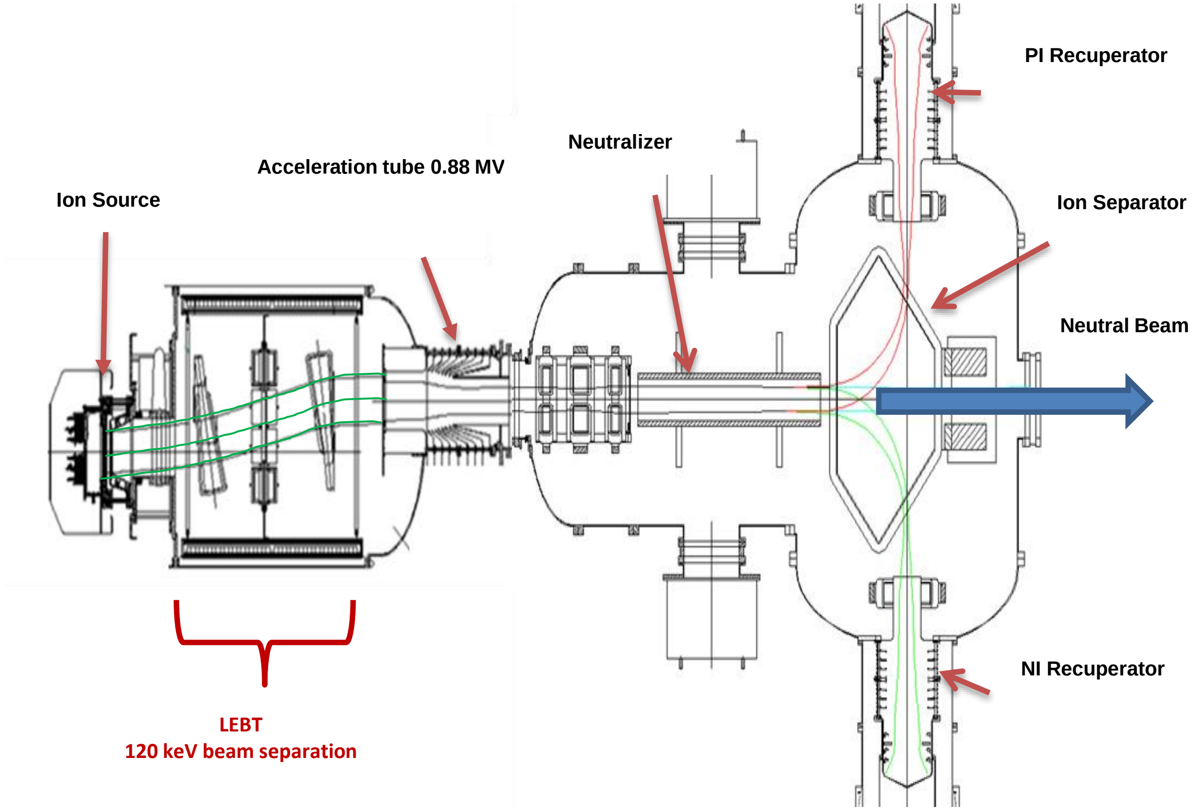

Elements of injector developing at BINP:

- **Multiaperture RF negative ion sources**
- **LEBT**
- **High energy accelerating tube**
- **Photodetachment and plasma neutralizers**
- **Wide-aperture separating magnet**
- **Energy recuperator.**

Negative-ion based Neutral Beam Injector

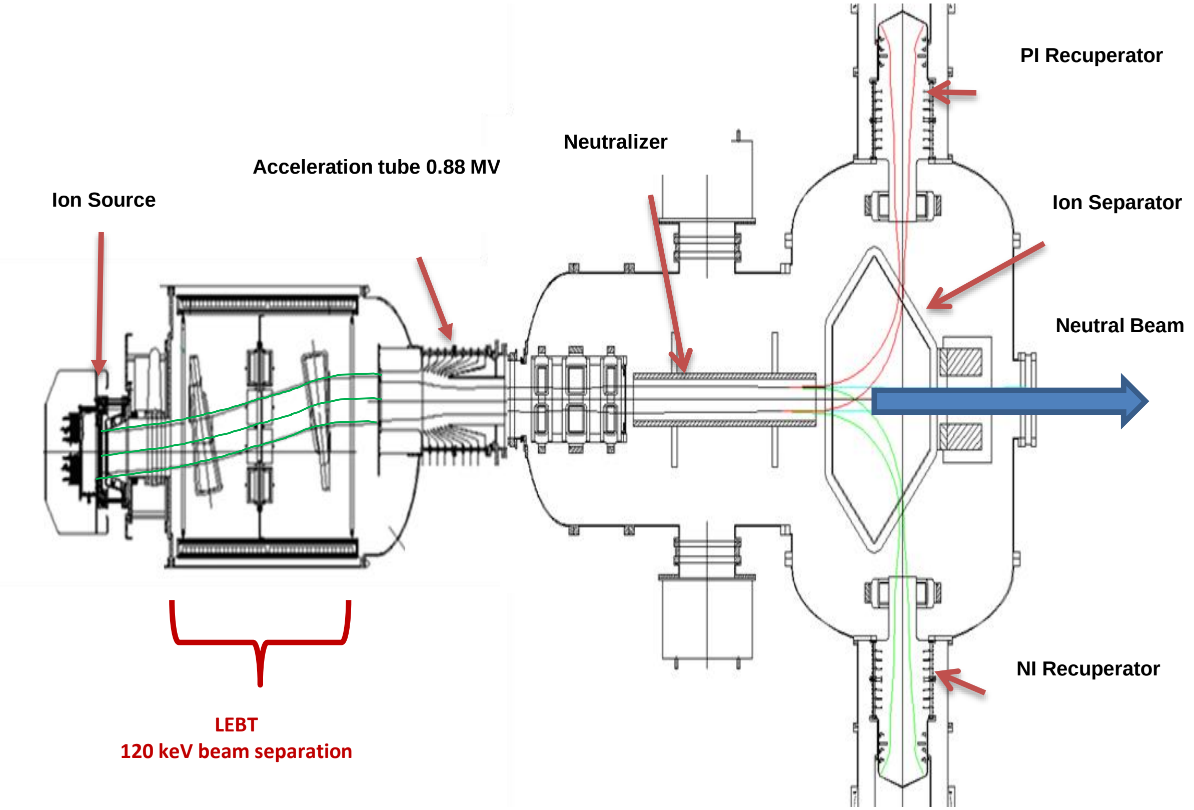

Beam acceleration is produced after purifying from the co-streaming fluxes of primary and secondary particles (gas, fast neutrals, electrons, cesium, light)

Negative ion beam is focused to a single-aperture 0.5-1 MeV accelerating tube. The stresses of the accelerator must be considerably reduced.

Test Stand

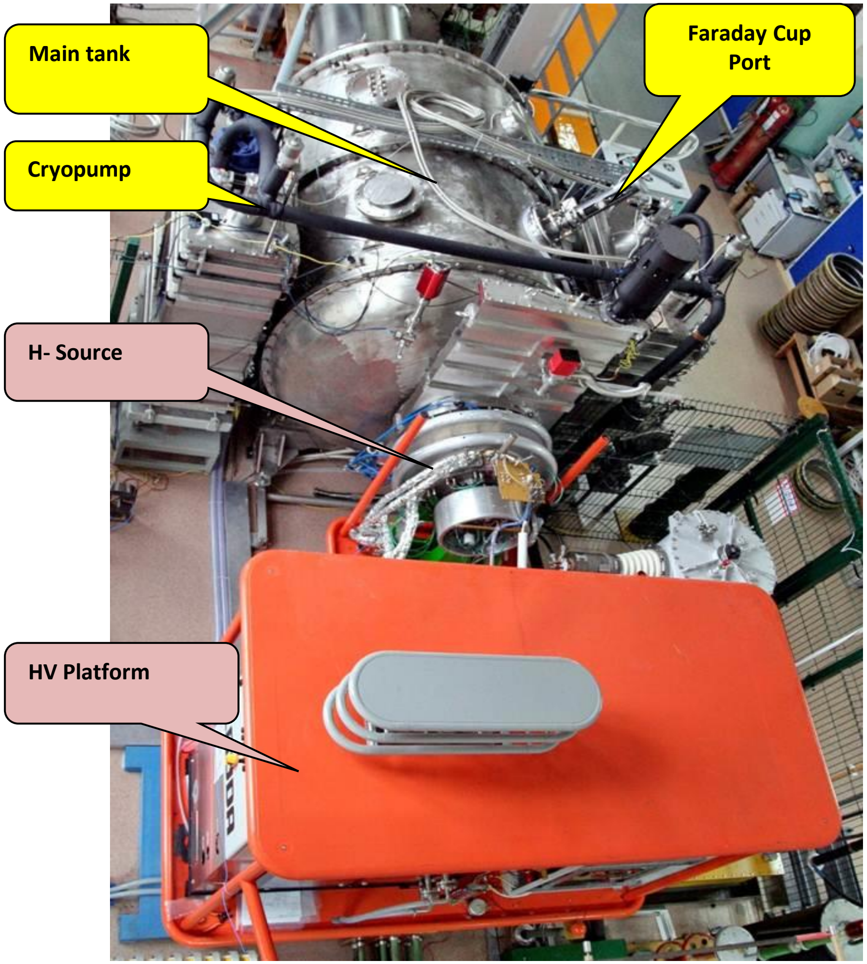

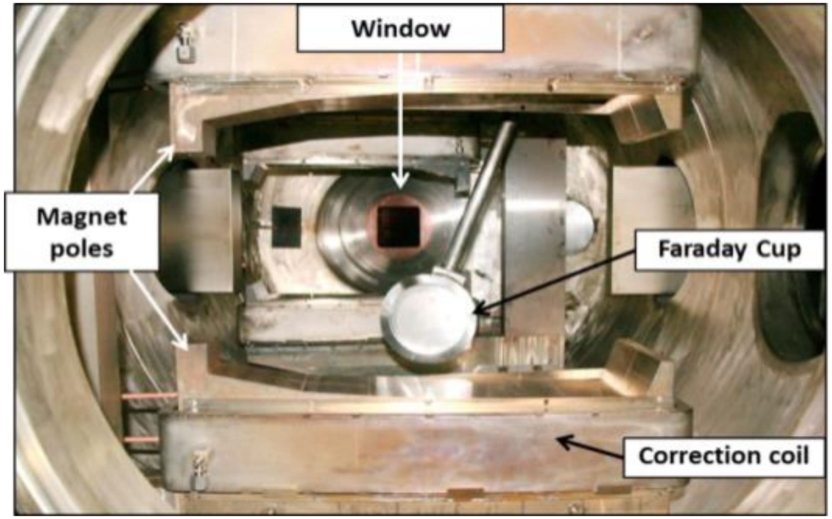

Test stand was designed for study:

- **Beam formation in RF negative ion source**
- **Beam transport through LEBT with two large-aperture bending magnets**

Beam measurements scheme

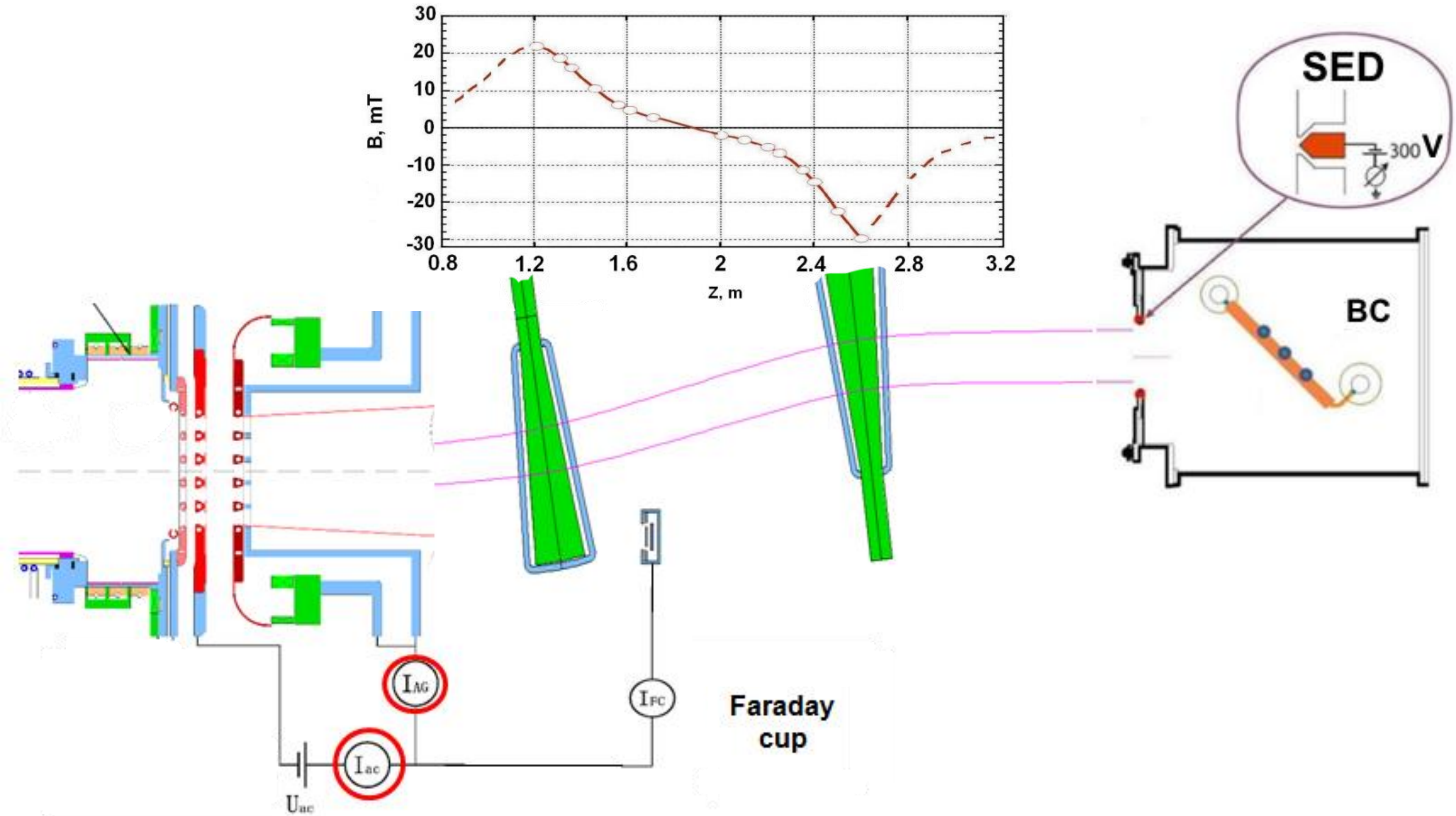

- H- beam was measured by Faraday Cup (at 1.6 m) and by calorimeter (at 3,5 m)
- IOS circuits currents I_{ac}, I_{AG} were measured to control H- beam current
- Transported H^- beam was scanned along calorimeter plane by change of magnet #1 and 2 field.

H- beam and co-extracted electron currents

1.2 A, 85 keV, 1.6 s shot

RF discharge power 36 kW

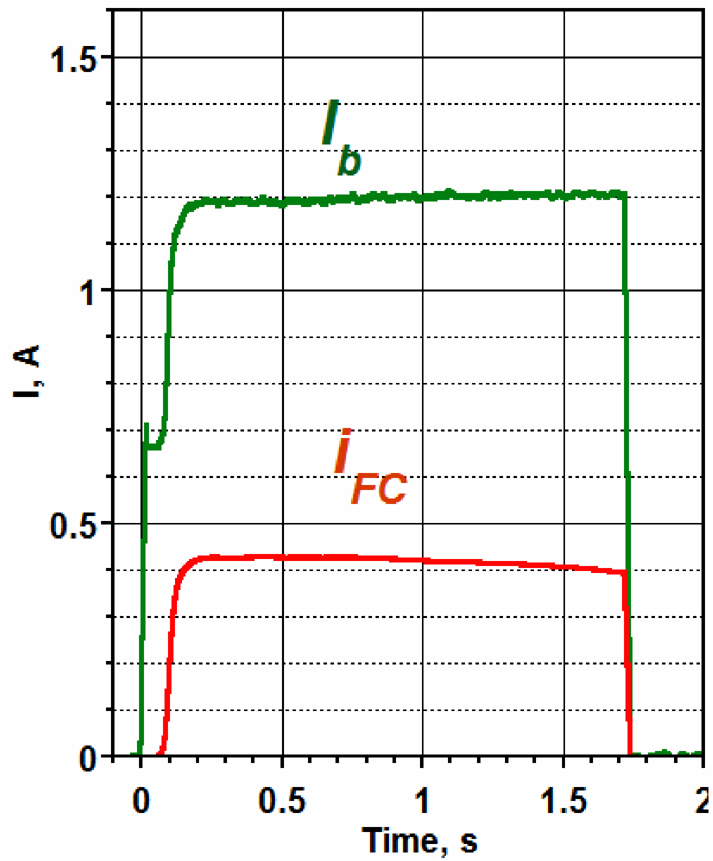

0.8 A, 100 keV, 12 s shot

RF discharge power 22 kW

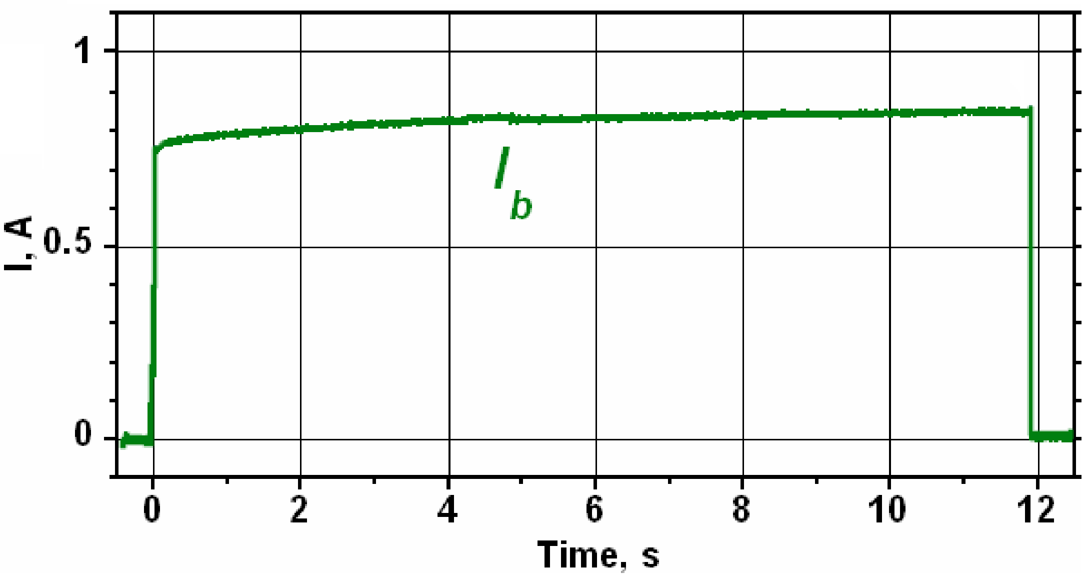

Beam current is stable during the long pulse

H- beam at distance 1.6 m

Comparison of outgoing beam current I_b and beam current I_{FC}, transported to FC plane

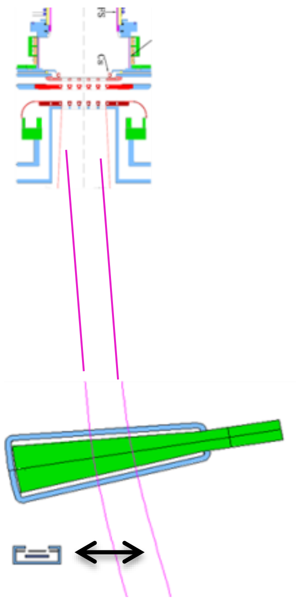

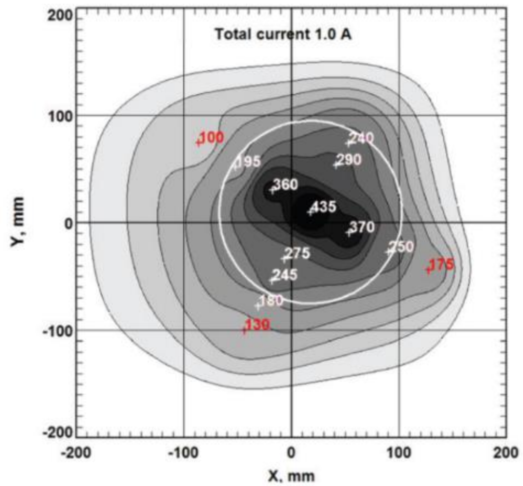

Beam profile for current at FC plane ~ 1 A

Divergence ± 60 x ± 50 mRad,

FC ø 170 mm

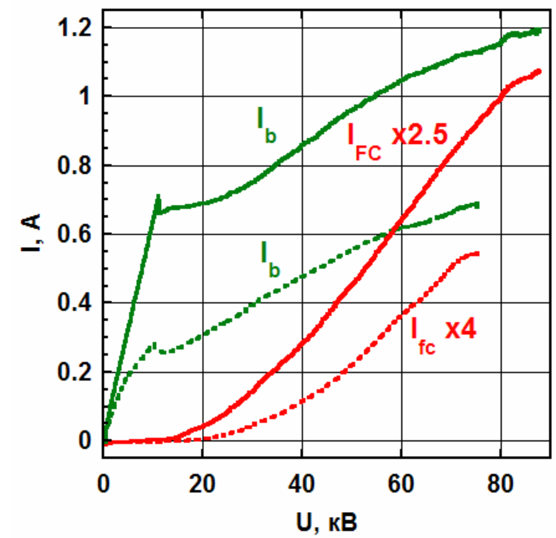

H- beam current I_b, outgoing the source and beam current I_{FC} at Faraday cup plane vs acceleration voltage.

Continuous – RF 35 kW, Uex 12 kV

Dashed – RF 25 kW, Uex 7.5 kV

- H- current I_{FC} is ~ 15 % smaller, than beam current I_b, outgoing from the source
- No saturation of I_b and I_{FC} currents growth was recorded with beam energy up to 100kV.
- Currents rise with energy growth is caused by improved transmission, by decrease of H- ions stripping and by beam focusing to FC

H- beam at distance 1.6 m

Dependences *vs* hydrogen filling pressure

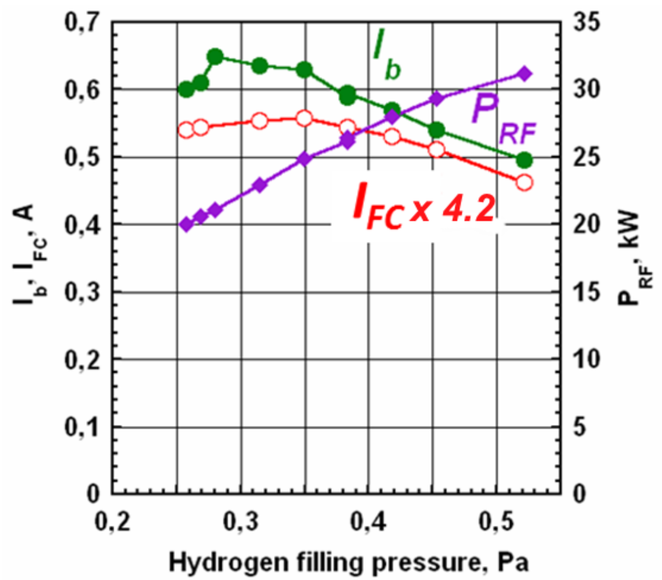

Normalizing to RF discharge power 25 kW

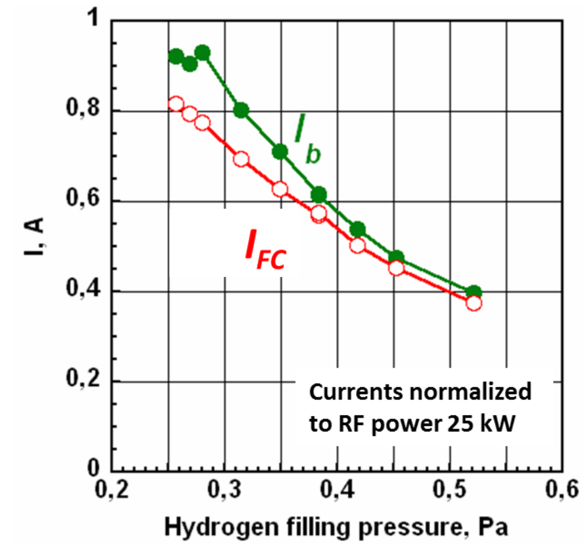

The similar decrements for I_b and I_{FC} currents vs H_2 shows the dominant stripping of H- ions in the AG+GG area .

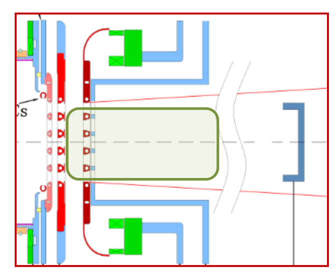

Beam transport to calorimeter

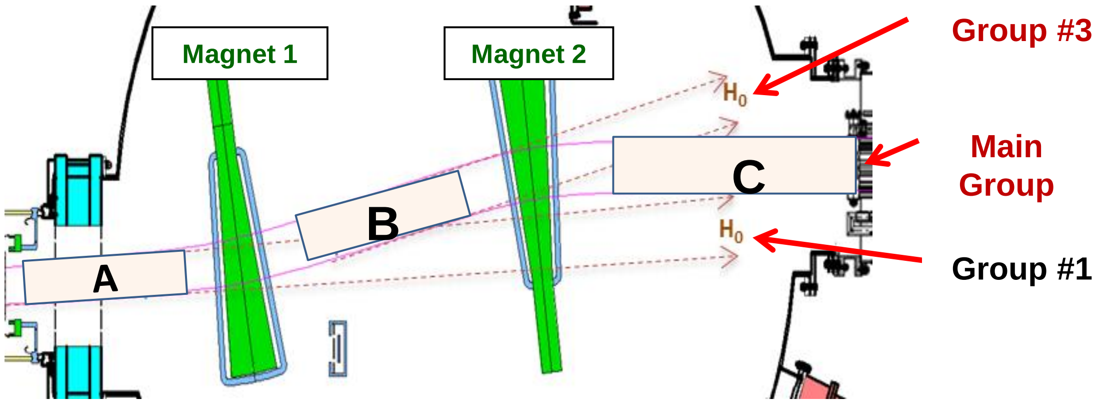

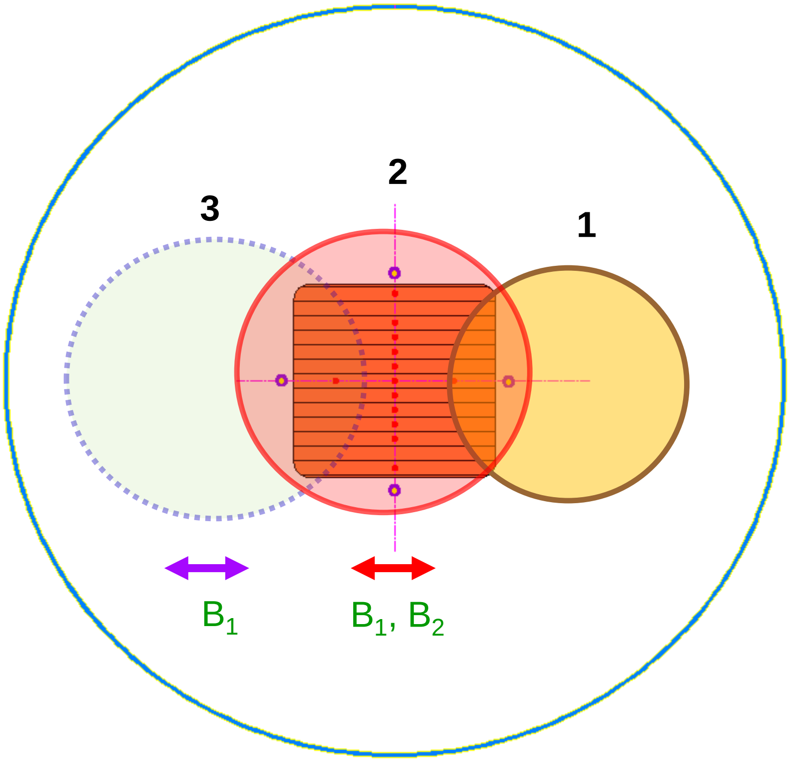

Main Group consists of H- beam + neutrals, produced by H- stripping in section C
Group # 3 is produced by H- ions stripping in section B, after ions bending by magnet 1

Main Group (2) and Group #3 are shifted with magnets field change

Group 1 is produced by H- ions stripping in section A, before H- ions bending by magnets. It is not shifted by magnets field

H- beam transport to calorimeter

Small income of neutral beam satellites were displayed at tank vacuum $3 \cdot 10^{-3}$ Pa

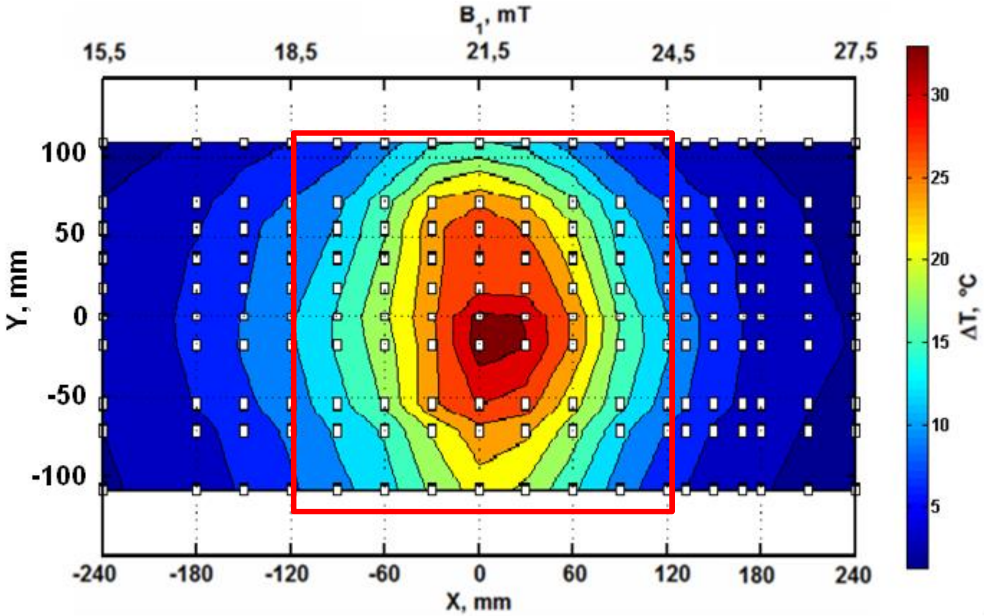

1,2 A, 93 kV, $3 \cdot 10^{-3}$ Pa

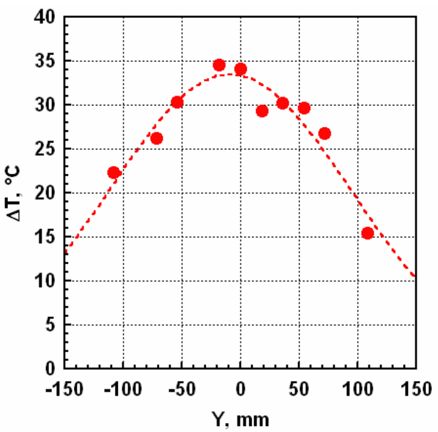

At X=0

~ 60% of H- beam, outgoing the source were transported to calorimeter area 24 x 24 cm² (measured within red rectangular)

~ 80% of H- beam, outgoing the source were transported to calorimeter area 48 x 24 cm² at energy 93 кeV (measured by beam shift)

X- profile of transported H- beam

1,2 A, 93 kV, $3 \cdot 10^{-3}$ Pa

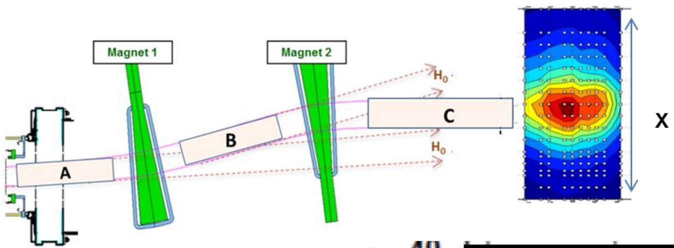

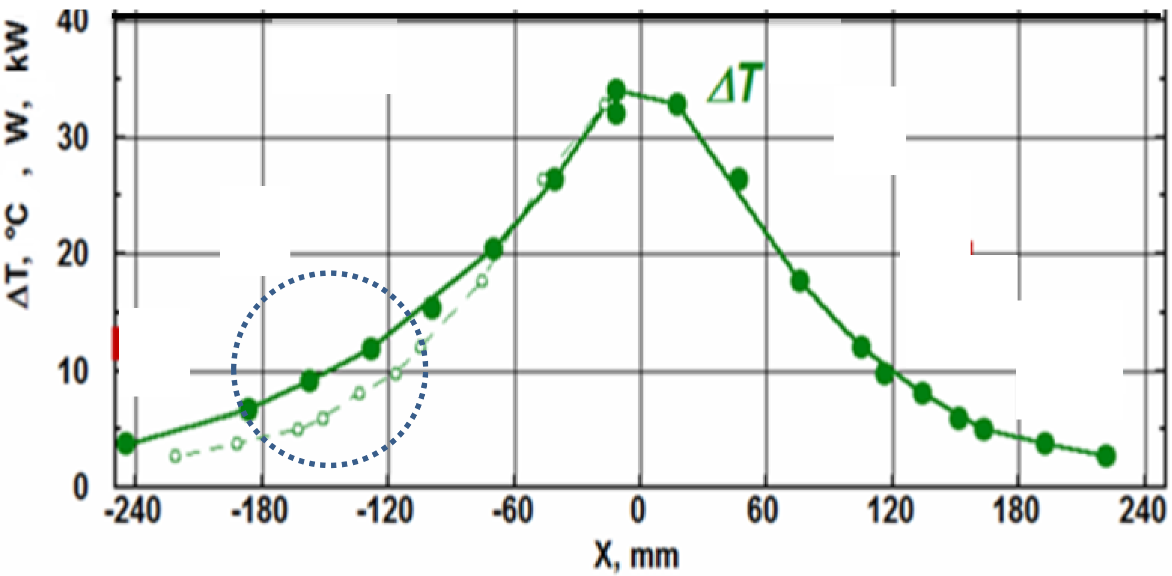

ΔT - temperature rise of central thermocouple vs H- beam shift during magnetic scan.

X- profile shows the structure of beam main group.
Profile asymmetry indicates a few income of atomic group #3

Power to calorimeter W *vs* X-shift

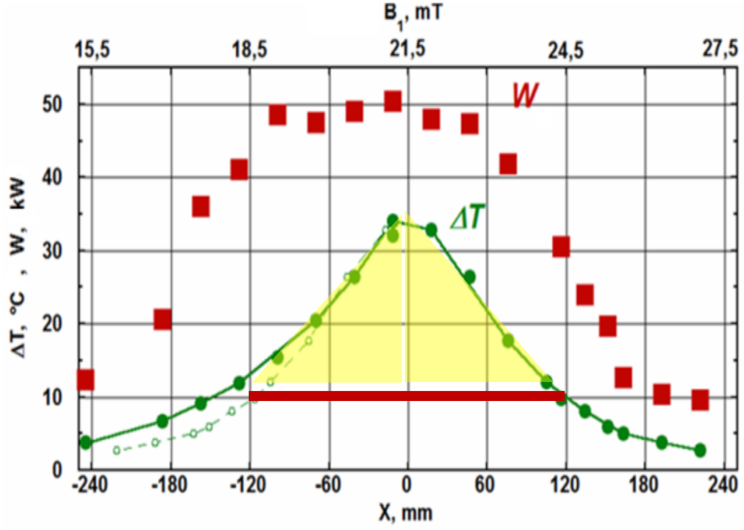

1,2 A, 93 kV, $3\cdot10^{-3}$ Pa

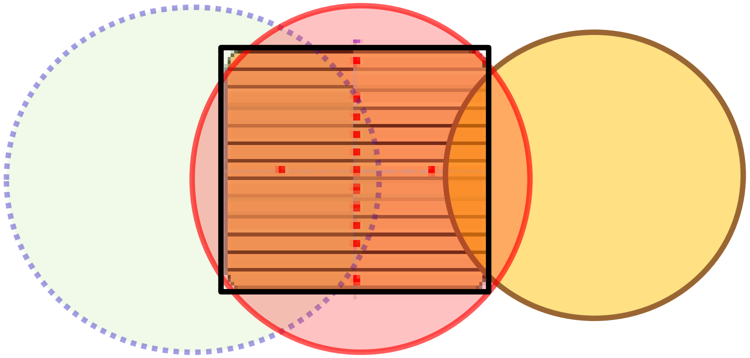

Power to calorimeter W *vs* X-shift

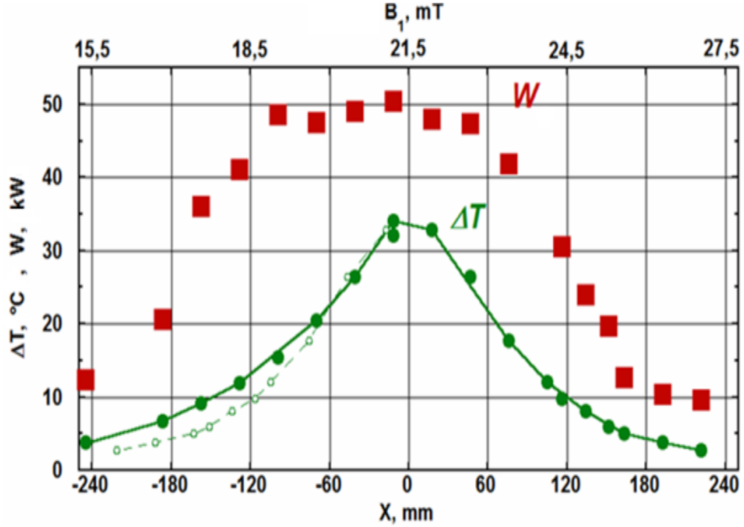

1,2 A, 93 kV, 3·10^{-3} Pa

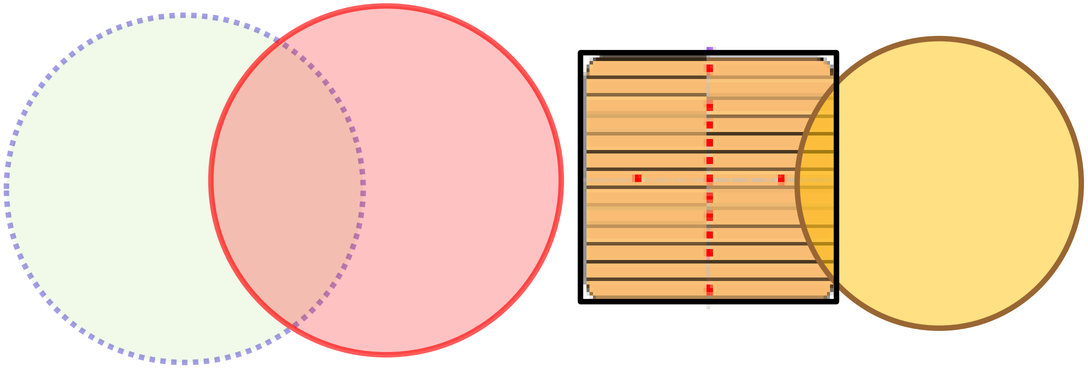

Composition of beam, entering calorimeter window at B_1= 27,5 mT B_2=21 mT

~2 kW atomic group #1 galo

Power to calorimeter W *vs* X-shift

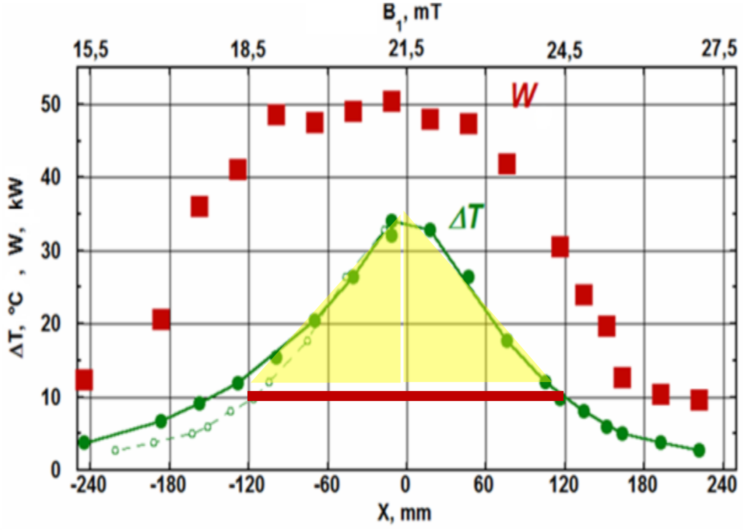

1,2 A, 93 kV, $3{\cdot}10^{-3}$ Pa

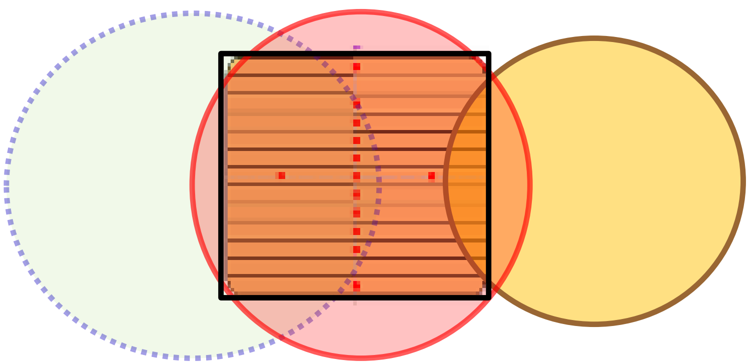

Composition of 50 kW beam, entering calorimeter window at B_1= 21,5 mT

47 kW main group, 1 kW group #3, ~2 kW atomic group #1 galo

Power to calorimeter W *vs* X-shift

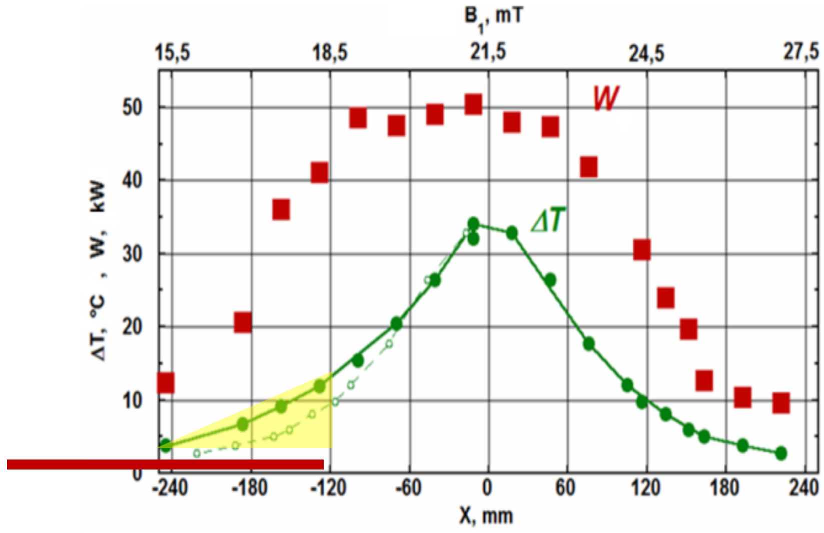

1,2 A, 93 kV, $3\cdot10^{-3}$ Pa

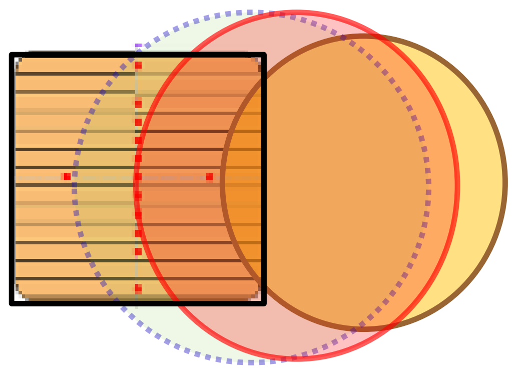

Composition of 12 kW beam, entering calorimeter window at B_1= 15,5 mT
7 kW - left side of main group, 3 kW – left half of group #3, ~2 kW atomic group #1 galo

Power to calorimeter W *vs* X-shift

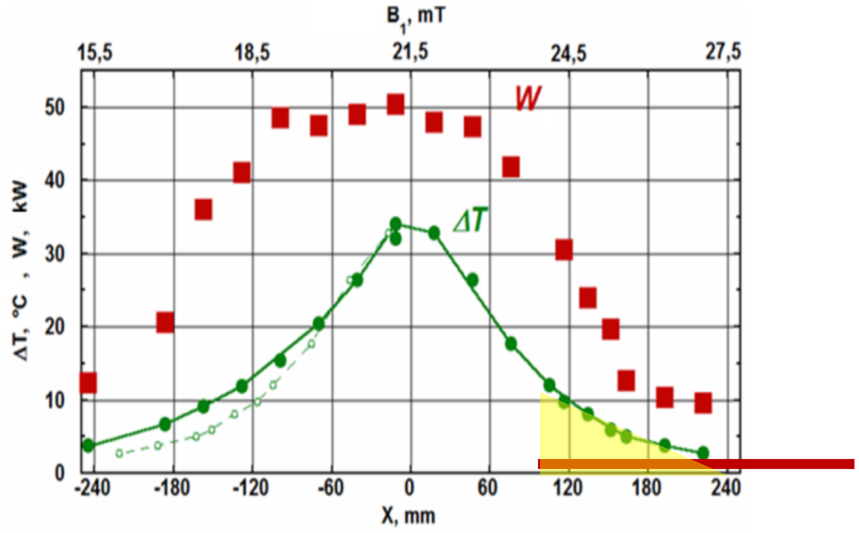

1,2 A, 93 kV, $3 \cdot 10^{-3}$ Pa

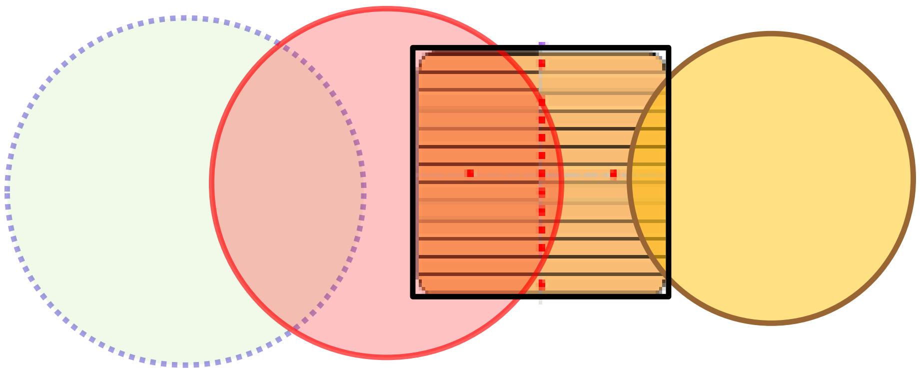

Composition of 10 kW beam, entering calorimeter window at B_1= 27,5 mT

8 kW - right part of main group, ~2 kW atomic group #1 galo

H- ions stripping at poor vacuum

Neutral Group #3 is clearly displayed at poor tank vacuum $7 \cdot 10^{-3}$ Pa

0.6 A, 82 kV, $7 \cdot 10^{-3}$ Pa

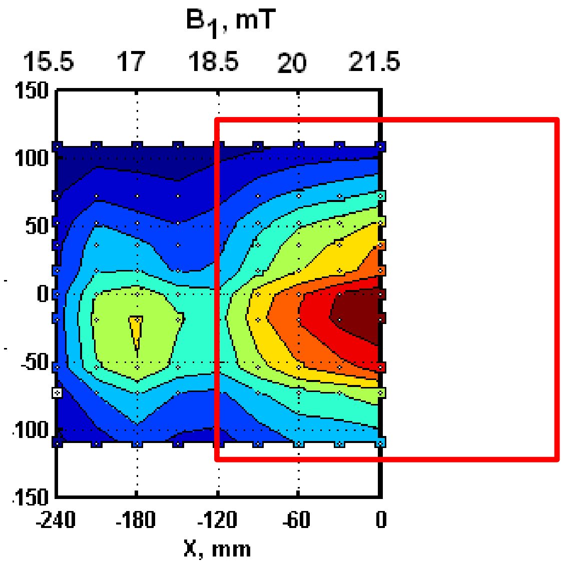

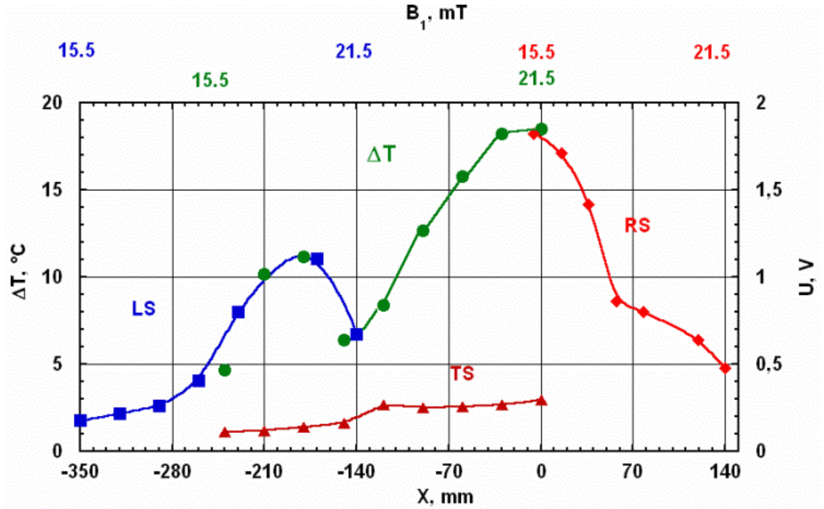

H- beam is separated from atomic Groups #1 and #3

X-distribution of the beam along calorimeter
ΔT- temperature rise of central thermocouple
LS , RS, TS- secondary electron emission detectors

At poor vacuum ~ 50% of H- ions beam enter the calorimeter window 24x24 cm²

SEDs Oscillogram

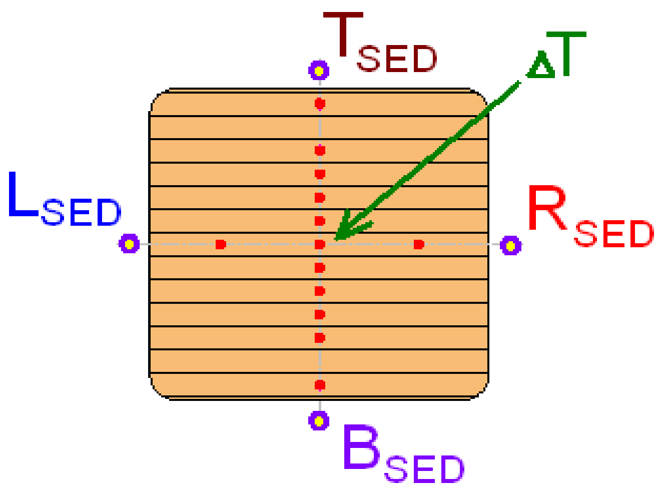

Left, Top, Right and Bottom SED positions at the periphery of calorimeter window

0.6 A, 82 kV, $7{\cdot}10^{-3}$ Pa

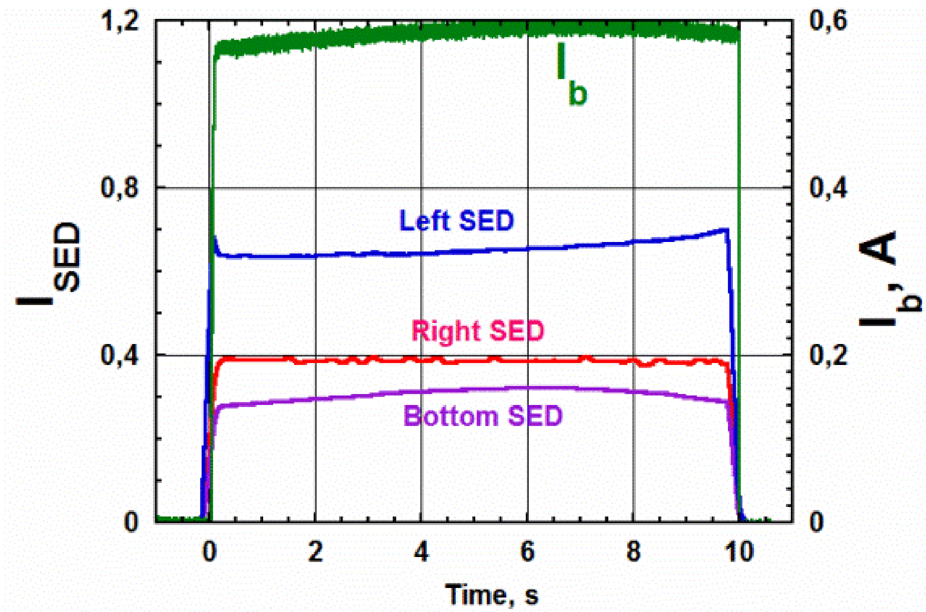

Beam main group is focused to the calorimeter center

- **Left SED** **shows little increase of atomic group #3 to the 10 s shot end**
- **Bottom SED** **shows a decrease of H- group to the pulse end (similar to those for the outgoing beam** I_b**) .**
- **RIGHT SED** **is stable during the pulse**

Y-profile of beam main group at calorimeter

At tank vacuum 3·10^{-3} Pa

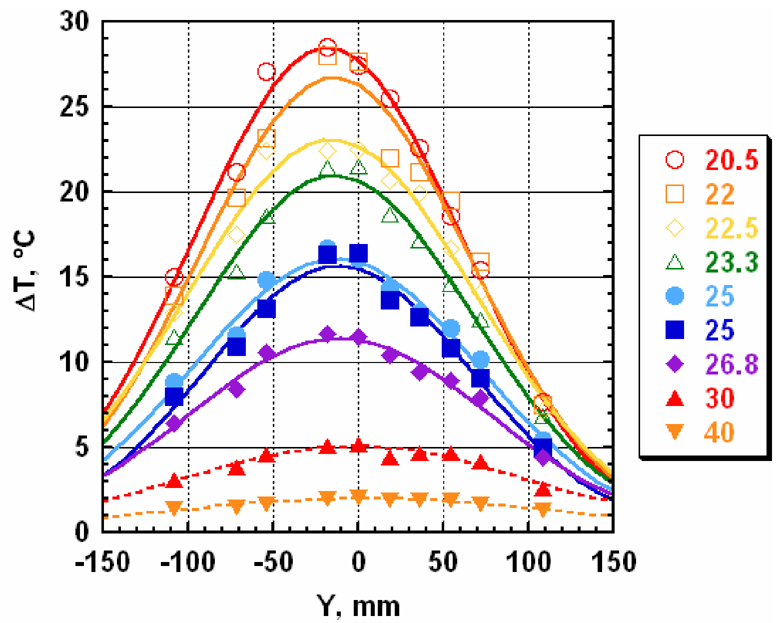

Y-profile (X=0) *vs* plasma grid potential

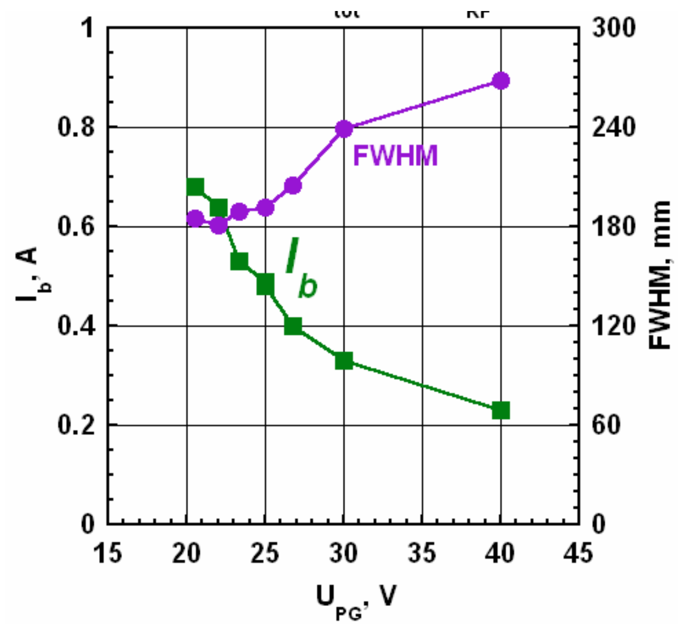

Beam FWHM *vs* plasma grid potential

Changing U_{PG} = 20-25 V doesn't depend on beam size at 3.5 m

Y-profile of beam main group at calorimeter

At tank vacuum 3·10^{-3} Pa

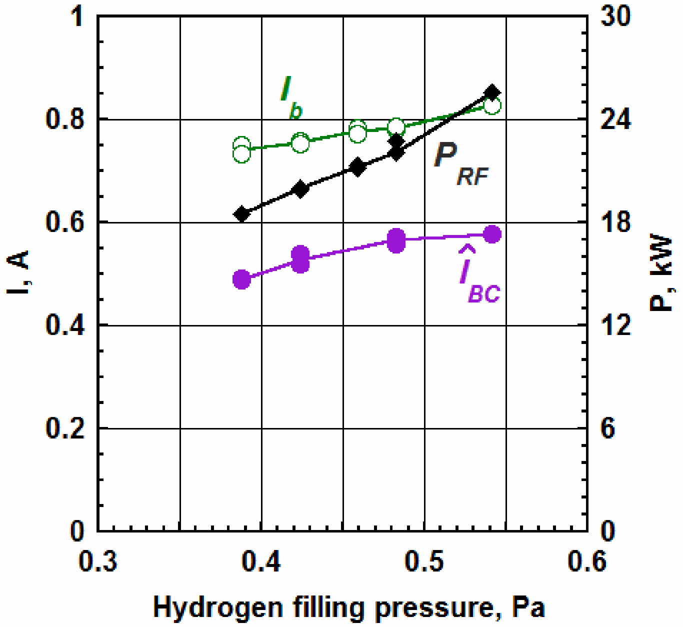

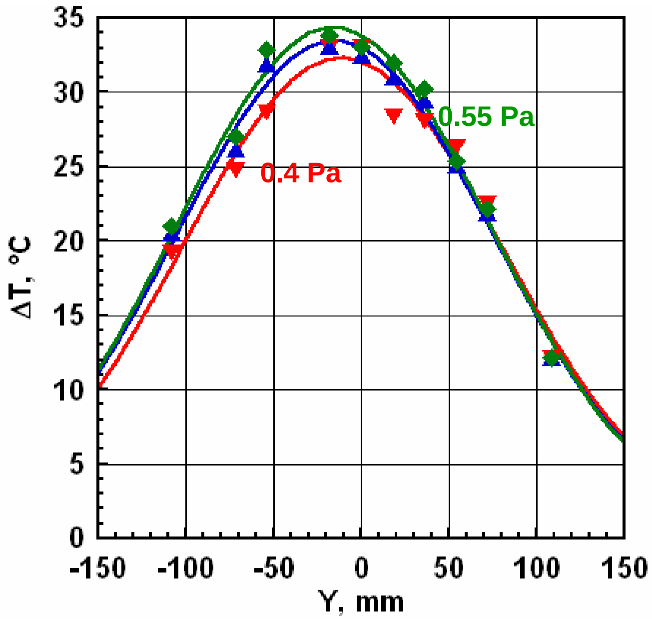

Y-profile *vs* hydrogen filling pressure

Y-profile of beam main group at calorimeter

At tank vacuum 3·10^{-3} Pa

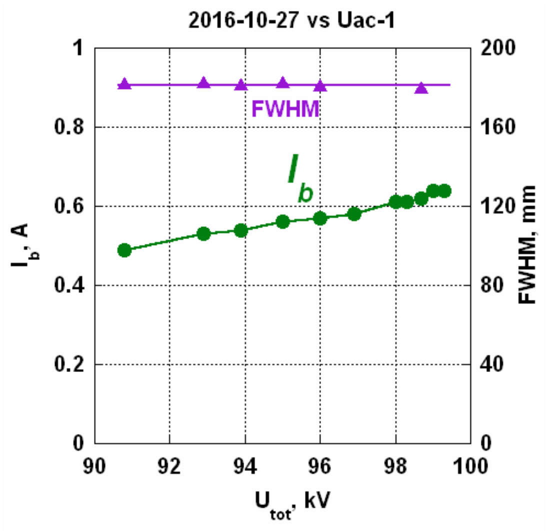

Beam FWHM *vs* beam energy

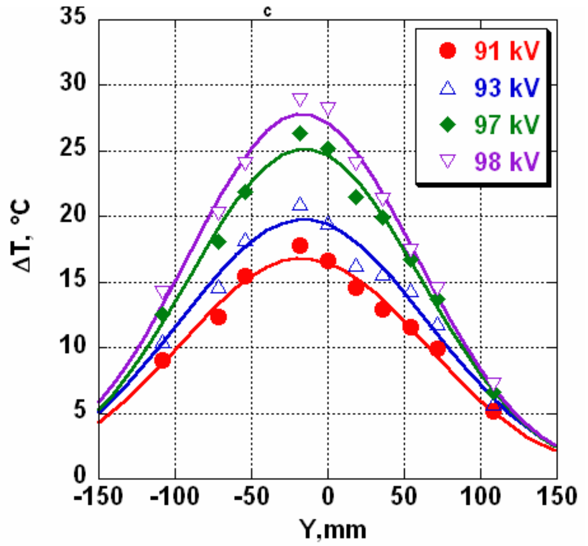

Y- profile *vs* beam energy

Beam transport efficiency

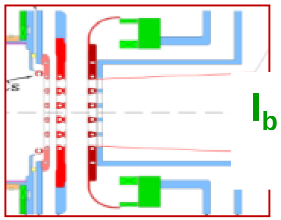

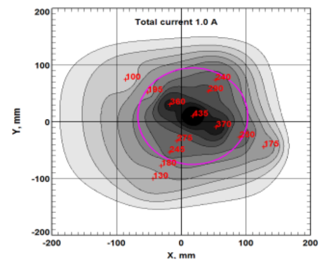

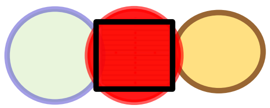

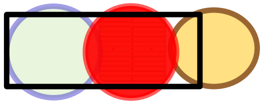

Measurement points	At IOS exit	At FC plane		At BC plane 48 x 24 cm^2		In window 24x24 cm^2
Beam Groups	NI beam	NI beam	group 1	Group 2 + 3	Group 1	Group 2 + 1
Case #1	0.9A·93kV=84 kW	72 kW	12 kW	68 kW	2 kW	50 kW
Case #2	0.6A·80kV=48kW	40 kW	8 kW	28 kW	-	24 kW

At optimal vacuum ~ 80% of H- ions beam enter the calorimeter area 48x24 cm^2

At typical operation vacuum in the tank $3 \cdot 10^{-3}$ Pa, beam losses in the LEBT are mainly caused by stripping near the accelerating electrode of the IOS, and the group of neutrals obtained by stripping the beam in the region between the magnets is practically indistinguishable on the measured beam profile on the BC.